Autotrophic adaptive laboratory evolution of the acetogen *Clostridium autoethanogenum* delivers the gas-fermenting strain LAbrini with superior growth, products, and robustness

Henri Ingelman[a,*], James K. Heffernan[b,*], Audrey Harris[c,*], Steven D. Brown[c], Asfand Yar Saqib[a], Marina J. Pinheiro[a,1], Lorena Azevedo de Lima[a], Karen Rodriguez Martinez[b], Ricardo A. Gonzalez-Garcia[b], Grant Hawkins[c], Jim Daleiden[c], Loan Tran[c], Hunter Zeleznik[c], Rasmus O. Jensen[c], Vinicio Reynoso[c], Séan D. Simpson[c], Michael Köpke[c], Esteban Marcellin[b,#], Kaspar Valgepea[a,#]

[a]ERA Chair in Gas Fermentation Technologies, Institute of Technology, University of Tartu, 50411 Tartu, Estonia

[b]Australian Institute for Bioengineering and Nanotechnology (AIBN), The University of Queensland, 4072 St. Lucia, Australia

[c]LanzaTech Inc., 60077 Skokie, USA

*These authors contributed equally to this work.

[1]Present address: Libbs Farmacêutica, 01140-050 São Paulo, Brazil

[#]Correspondence: Esteban Marcellin, e.marcellin@uq.edu.au; Kaspar Valgepea, kaspar.valgepea@ut.ee

ABSTRACT

Microbes able to convert gaseous one-carbon (C1) waste feedstocks are of growing importance in transitioning to the biosustainable production of renewable chemicals and fuels. Acetogens are particularly interesting biocatalysts since gas fermentation using *Clostridium autoethanogenum* has already been commercialised. Most non-commercial acetogen strains, however, need complex nutrients, display slow growth, and are not sufficiently robust for routine bioreactor fermentations. In this work, we used three adaptive laboratory evolution (ALE) strategies to evolve the wild-type model-acetogen *C. autoethanogenum* to grow faster, without complex nutrients and to be robust in operation of continuous bioreactor cultures. Seven evolved strains with improved phenotypes were isolated on minimal medium with one strain, named "LAbrini" (LT1), exhibiting superior performance in terms of the maximum specific growth rate, product profile, and robustness in continuous cultures. Differing performance of the strains between bottle batch and continuous cultures shows the importance of testing novel strains in industrially relevant continuous fermentation conditions. Interestingly, a very distinct transcriptome profile linked to a potential CO toxicity phenotype was observed in bioreactor cultures for one evolved strain. Whole-genome sequencing of the seven evolved strains identified 25 mutations with two genomic regions under stronger evolutionary pressure. Our analysis also suggests that the genotypic changes that are potentially responsible for the improved phenotypes may serve as useful candidates for metabolic engineering of cell factories. This work provides the robust *C. autoethanogenum* strain LAbrini to the academic community to speed up phenotyping and genetic engineering, improve quantitative characterisation of acetogen metabolism, and facilitate the generation of high-quality steady-state datasets.

Keywords: adaptive laboratory evolution, gas fermentation, chemostat, metabolomics, whole-genome sequencing, RNA sequencing.

1. INTRODUCTION

The continuously increasing emissions of one-carbon (C1) gases (CH_4, CO_2, CO) (IEA, 2022) from burning fossil fuels are the main drivers behind climate change. Alarmingly, this continuing trend might lead to irreversible climate change and a great loss of biodiversity (IPCC, 2021). To tackle and possibly reverse these horrific trends, a circular bioeconomy with decarbonised energy sectors, sustainable chemical and fuel production, and integrated waste management needs to replace our linear take-make-waste economy (Kircher, 2021). While solar and wind are leading the way for decarbonising energy generation, the improvement of various biocatalysts allowing the "up-cycling" of waste C1 feedstocks is considered one of the key strategies for sustainable production of chemicals and fuels towards achieving carbon neutrality (Zhang et al., 2022).

One attractive route toward recycling waste carbon into products is gas fermentation (Fackler et al., 2021). The ideal biocatalysts for this bioprocess are bacteria termed acetogens that use the energy-efficient Wood–Ljungdahl pathway (WLP) to fix carbon oxides (CO_2 and CO) into acetyl-CoA from a wide range of feedstocks (Pavan et al., 2022). Notably, the model-acetogen *Clostridium autoethanogenum* is already used in commercial-scale ethanol production (Köpke and Simpson, 2020) and has been successfully piloted for acetone and isopropanol production (Liew et al., 2022). However, advancing understanding of acetogen metabolism and rational metabolic engineering of cell factories by the academic community has been slowed down by the fact that non-commercial acetogen strains struggle to grow on minimal medium, show slow gas uptake and growth, and are challenging to run in continuous bioreactor cultures. Use of minimal growth medium (e.g. without yeast extract [YE]) is required for accurate quantification of carbon distribution and metabolic modelling to understand metabolism and predict phenotypes (Valgepea et al., 2018, 2017b). Faster gas uptake and growth would speed up phenotyping and genetic engineering of acetogens (Bourgade et al., 2021; Pavan et al., 2022). A more robust strain in terms of operating continuous bioreactor cultures (Klask et al., 2020; Mahamkali et al., 2020) would ease the generation of high-quality steady-state data. Also, the use of various *C. autoethanogenum* strains for academic research complicates comparability of results that could be improved by the use of a common and user-friendly strain. A publicly available acetogen strain with the above mentioned, improved features would strongly benefit the academic community.

Adaptive laboratory evolution (ALE) is a powerful and elegant approach for obtaining strains with improved traits as evolution's reliance on natural selection to enrich for mutants with increased fitness allows strain optimisation to be performed without requiring *a priori* knowledge of the

genetic alterations necessary to effect such changes (Sandberg et al., 2019). It has recently been used also for engineering and improving autotrophic growth capabilities. For example, ALE was used to convert the natively heterotrophic workhorse microbes *Escherichia coli* (Gleizer et al., 2019) and *Pichia pastoris* (Gassler et al., 2019) to CO_2-fixing organisms. In acetogens, ALE has improved tolerance towards methanol in *Sporomusa ovata* (Tremblay et al., 2015), cyanide in *Clostridium ljungdahlii* (Oswald et al., 2018), benzene, toluene, and xylenes in *C. autoethanogenum* (Piatek et al., 2020), and acetate in *Clostridium* sp. AWRP (Kwon et al., 2022). ALE also afforded an *Eubacterium limosum* strain with higher CO tolerance and faster growth (Jin et al., 2022; Kang et al., 2020). Additionally, *C. ljungdahlii* and *C. autoethanogenum* have been adapted by continuous bioreactor cultivation to grow without YE (Martin et al., 2015; Schulz et al., 2023), but it is not clear if the phenotype was the result of adaptation (i.e. reversible) or evolution (i.e. permanent).

In this work, we used ALE intending to acquire superior *C. autoethanogenum* strains that would grow faster, without YE on minimal medium, and show robustness for operating continuous bioreactor cultures. Seven evolved strains with improved phenotypes were isolated across three different ALE strategies with one strain – named "LAbrini" (LT1) – exhibiting superior performance in terms of maximum specific growth rate (μ_{max}), product profile, and robustness in bioreactor cultures. Genome sequencing revealed 25 mutations with two genomic or "hot-spot" regions across the seven evolved strains and suggested genotypic changes potentially responsible for the improved phenotypes. This work provides the robust *C. autoethanogenum* strain LAbrini to the academic community to speed up phenotyping and genetic engineering, improve quantitative characterisation of acetogen metabolism, and facilitate the generation of high-quality steady-state datasets.

2. MATERIALS AND METHODS

2.1. Starting bacterial strain for adaptive laboratory evolution (ALE)

The starting strain for all three ALEs (see next section) was *Clostridium autoethanogenum* strain JA1-1 (Abrini et al., 1994) deposited in the German Collection of Microorganisms and Cell Cultures (DSMZ) as DSM 10061 and stored as a glycerol stock at −80°C.

2.2. Three adaptive laboratory evolution (ALE) workflows

2.2.1. University of Tartu (UT) ALE workflow – bottle ALE on CO

Glycerol stock of DSM 10061 was revived in PETC-MES medium (Valgepea et al., 2017b) supplemented with 5 g/L of fructose, 1.5 g/L of YE, and 0.4 g/L of cysteine-HCl·H_2O as the reducing agent. Cells were sub-cultured from exponential growth phase into the same medium but with

fructose replaced by CO as the carbon source: this culture was Round 1 of UT ALE (Fig. 1a). Cells were then sub-cultured from exponential growth phase to the same medium with CO (Round 2). Starting from Round 3, each round was carried out in 2□4 replicate bottles and the culture with the fastest growth was sub-cultured to the next round from exponential growth phase. Additionally, during Rounds 3□5, YE was removed from the medium in a stepwise manner: first to 0.5 g/L (Round 3), then to 0.05 g/L (Round 4), and no YE starting from Round 5 of UT ALE. Serial sub-culturing was stopped after 35 rounds when the decrease of maximum specific growth rate (μ_{max}) during UT ALE had levelled off (Fig. 1b).

Bottle cultivations were carried out with 50 mL medium in 250 mL Schott bottles incubated horizontally at 37°C with orbital shaking at 120 RPM under strictly anaerobic conditions. Culture bottle headspace was pressurised to 140 kPa with a 60% CO and 40% Ar gas mixture (AS Eesti AGA). Additionally, a "swap ALE" was performed where the culture was transferred between the previous CO mixture and syngas (50% CO, 20% CO_2, 20% H_2, 10% Ar; AS Eesti AGA) (Supplementary Fig. 1). Growth was tracked by measuring culture optical density (OD) at 600 nm and μ_{max} was calculated using 3□5 data points from the exponential phase (except for a few cultures using two data points indicated on Fig. 1b) that yielded a correlation coefficient $R^2 > 0.98$ between culture time and natural logarithm (ln) of OD. At the time of sub-culturing, cultures were sampled for extracellular metabolome analysis and occasionally glycerol stocks were prepared.

Glycerol stocks made from Round 26 (110 generations; blue marker on Fig. 1b) and 35 (142 generations; yellow marker on Fig. 1b) were used to obtain single colony isolates by plating the mixed populations on Round 1 medium with agar (12 g/L) and incubation at 37°C under autotrophic conditions (same gas mixture as for UT ALE). Ten colonies were screened in bottles under the same conditions as in Round 5 of UT ALE (e.g. CO without YE) and three isolates named UT1 (from Round 26) and UT2 and UT3 (from Round 35) were selected for further characterisation (see below) based on μ_{max}, or ethanol or 2,3-butanediol (2,3-BDO) yields per biomass (see Results for details). The latter yields (mmol of product/gram of dry cell weight [gDCW]) were estimated by linear regression between the respective product (mmol/L) and biomass concentrations (gDCW/L) that were measured during exponential growth phase with correlation coefficients $R^2 > 0.95$.

2.2.2. University of Queensland (UQ) ALE workflow – bottle and bioreactor ALE on syngas

Glycerol stock of DSM 10061 was revived in the same medium as in Round 1 of UT ALE and the bottle was pressurised to 125 kPa with CO_2. Cells were sub-cultured in single replicate bottles from exponential growth phase into the same medium but with a gradual reduction of fructose (i.e. 2.5, twice 1, and 0 g/L), with 190 kPa syngas (50% CO, 20% CO_2, 20% H_2, 10% Ar; BOC Australia) replacing

the carbon source (Series 1 of UQ ALE). Next, YE was gradually removed from the medium over 8 bottles (i.e. twice 1.5, twice 1, 0.5, twice 0.25, and 0 g/L) and the first YE-free culture was glycerol stocked before pausing the ALE experiment (Series 2 of UQ ALE; grey markers in Fig. 1d). The latter glycerol stock was revived in the same medium as in Round 1 of UT ALE and bottle pressurised to 140 kPa with syngas before sub-culturing in YE-free medium 3-times with 190 kPa and 4-times with 140 kPa syngas (Series 3 of UQ ALE; orange markers in Fig. 1d).

Bottle cultivations were carried out with either 25 or 100 mL medium (125 or 500 mL bottles) and incubated horizontally at 37°C with orbital shaking at 200 RPM under strictly anaerobic conditions. Growth was tracked by measuring culture OD at 600 nm and μ_{max} was calculated using 3 data points from the exponential phase that yielded a correlation coefficient $R^2 > 0.99$ between culture time and ln of OD. At the time of sub-culturing, glycerol stocks were occasionally prepared.

The final culture of Series 3 was used as the inoculum for a bioreactor ALE experiment, where the culture was grown on syngas predominantly under chemostat operation at pH 5 (Valgepea et al., 2017a) while other parameters (e.g. dilution rate, agitation, gas flow rates) were varied based on culture growth (Series 4 of UQ ALE; blue markers in Fig. 1d). After obtaining steady states at high biomass concentrations and ~2,300 h of fermentation, the bioreactor culture was plated on solid medium (Round 1 of UT ALE medium with 12 g/L agar) and incubated at 37°C under autotrophic conditions to obtain single colonies. Initially, pure CO at 70 kPa was used, but since only a few colonies appeared after 12 days, the headspace was replaced with syngas, and plates were incubated for a further 7 days after which 12 colonies were screened in bottles under the same conditions as at the end of Series 2 and 3 of UQ ALE (e.g. syngas without YE). Three isolates named UQ1, UQ2, and UQ3 were selected for further characterisation (see below) based on μ_{max}, or ethanol or 2,3-BDO yields per biomass (see Results for details). The latter yields (mmol of product/gDCW) were estimated with individual replicate (single colony revival) product (mmol/L) and biomass concentrations (gDCW/L), measured during the mid-/late-exponential growth phase.

2.2.3. LanzaTech (LT ALE) workflow – chemical mutagenesis and bioreactor ALE on syngas

Glycerol stock of DSM 10061 was revived in the same medium as in Round 1 of UT ALE and cultured using anaerobic techniques as described previously (Liew et al., 2022). Chemical mutagenesis was performed by growing cells anaerobically in bottles at 37°C with shaking until mid-exponential growth phase and then exposing cells to the chemical mutagen N-methyl-N'-nitro-N-nitrosoguanidine (NTG) as described before (Otte et al., 2009), except that after treatment cells were washed with anaerobic medium lacking YE and then transferred and cultured in a chemostat. Bioreactor chemostat gas fermentation with *C. autoethanogenum* has been described before (Liew

et al., 2022) and for selection and adaptation via gas fermentation no YE was added to the medium. The culture was grown for approximately 50 days to a final dilution rate (D) of 1 day^{-1} on the gas mixture of 53% CO, 7% H_2, 15% CO_2, and 25% N_2 before single colony isolation and glycerol stock preparation.

2.3. Characterisation of single colonies from evolved cultures

2.3.1. Bottle experiments

We carried out additional bottle experiments for more accurate characterisation of the single colonies isolated from the evolved cultures. We used the same conditions as for Round 5 in UT ALE (e.g. CO without YE) for UT and LT ALE isolates (UT1, UT2, UT3, LT1) and the same conditions as for Series 2 in UQ ALE (i.e., syngas without YE) for UQ and LT ALE isolates (UQ1, UQ2, UQ3, LT1). We also cultured the ALE starting strain DSM 10061 for comparison with YE (Round 2 conditions in UT ALE) and without YE (Round 5 conditions in UT ALE) on CO with UT ALE cultivation conditions. These cultures were sampled frequently from the exponential phase to enable a more accurate estimation of μ_{max} and product yields. μ_{max} was calculated using 3□12 data points from the exponential phase that yielded a correlation coefficient $R^2 > 0.99$ between culture time and ln(OD). Product yields for UT and LT isolates (mmol of product/gDCW) were estimated as described above with correlation coefficients $R^2 > 0.94$. For UQ isolates and LT1 on syngas, product yields were calculated from the difference of two time points in mid-exponential growth.

2.3.2. Bioreactor chemostat cultures

Cells were grown either on CO (60% CO and 40% Ar; AS Eesti AGA) for UT1, UT2 and UT3 or syngas (50% CO, 20% H2, 20% CO2, and 10% Ar; AS Eesti AGA) for UQ1 and LT1 in a chemically defined medium without YE as described before (Valgepea et al., 2017a). Cells were grown under strictly anaerobic conditions at 37°C and at pH 5 maintained by 5M NH4OH. Chemostat continuous cultures were performed in 1.4 L Multifors bioreactors (Infors AG) at a working volume of 750 mL connected to a Hiden HPR-20-QIC mass spectrometer (Hiden Analytical) for online high-resolution off-gas analysis. The system was equipped with peristaltic pumps; mass flow controllers (MFCs); pH, oxidation-reduction potential (ORP), and temperature sensors. Antifoam (435530; Sigma-Aldrich) was continuously added to the bioreactor at a rate of 10 µL/h to avoid foaming.

Chemostat cultures were run at D ~0.5, ~1, and ~2 day^{-1} (μ~0.02, ~0.04, and ~0.08 h^{-1}) across various isolates with variable gas-liquid mass transfer (gas flow rate and agitation) to maintain similar steady-state biomass concentrations (Table 1). In total, 25 steady-states were achieved after OD, gas uptake and production rates had been stable (<15% variability) for at least three working volumes. Bioreactor off-gas analysis using a mass spectrometer for determination of specific gas

uptake (CO and H_2) and production rates (CO_2 and ethanol) (mmol/gDCW/day) and determination of carbon recoveries and balances have been described before (Valgepea et al., 2017a).

2.4. Biomass concentration analysis

Biomass concentration in gDCW/L was determined by measuring culture OD at 600 nm and using the correlation coefficient between culture OD and DCW established at 0.23 (UT and LT ALE isolates) or 0.21 (UQ ALE isolates) using the methodology described before (Peebo et al., 2014).

2.5. Extracellular metabolome analysis

Analysis of exo-metabolome was performed using filtered broth samples stored at -20°C until analysis. Organic acids and alcohols were analysed by HPLC (Shimadzu Prominence-I LC-2030 plus system) using a Rezex™ ROA-Organic Acids H+ (8%) 300 ×7.8 mm column (00H-0138-K0; Phenomenex) and a guard column (03B-0138-K0; Phenomenex). Twenty microlitres of the sample were injected using an auto-sampler and eluted isocratically with 0.5 mM H2SO4 at 0.6 mL/min for 30 min at 45°C. Compounds were detected by a refractive index detector (RID-20A; Shimadzu) and identified and quantified using relevant standards using the software LabSolution (Shimadzu). We note that cells produced 2R,3R-butanediol.

2.6. Whole-genome sequencing (WGS) and mutation analysis

We performed whole-genome sequencing (WGS) for isolated clones UT1, UT2 and UT3 (UT ALE); UQ1, UQ2, and UQ3 (UQ ALE); LT1 (LT ALE); and also the ALE starting strain JA1-1 (DSM 10061) to ensure the accurate determination of mutations that appeared during ALE experiments. Genomic DNA for sequencing was extracted from exponential phase cultures of UT and UQ isolates using the MasterPure Gram Positive DNA Purification Kit (MGP04100; Biosearch Technologies) or Qiagen DNeasy Powersoil Pro Kit (47016; Qiagen) following the manufacturer's instructions. Genomic DNA for the LT1 strain was extracted with a phenol-chloroform extraction protocol. For UT and UQ isolates, purified DNA was quantified using the NanoDrop™ 1000 instrument (Thermo Scientific) or the Qubit 2.0 instrument (Invitrogen) before performing DNA sequencing using the MiSeq v2 Micro 300 cycles sequencing kit (MS-103-1002; Illumina) on the MiSeq sequencer (Illumina) with 2 × 151 bp paired-end dual indexed (2 × 8 bp) reads or using the Nextera DNA Flex Library Preparation Kit (20018705; Illumina) on the NovaSeq6000 sequencer (Illumina) with 2 x 150 bp paired-end reads. For LT1, DNA processing and sequencing was outsourced to third parties to generate 150 bp pair-end reads using the NovaSeq 6000 Illumina platform and continuous long reads from the PacBio Sequel II instrument, which were used to produce a genome assembly (see below).

WGS data analysis including trimming, filtering, mapping assembly, and annotation was carried out using the tool breseq version 0.37.0 (Deatherage and Barrick, 2014) with default settings for detecting missing coverage evidence and new sequence junctions and following parameters: limit fold coverage, 500; require match fraction, 0.95; polymorphism frequency cutoff, 1; polymorphism reject indel homopolymer length, 0; polymorphism reject surrounding homopolymer length, 0; polymorphism minimum variant coverage each strand, 1; polymorphism prediction base quality cutoff, 30; polymorphism minimum total coverage, 2; and polymorphism minimum total coverage each strand, 1. The total genome coverage, with paired-end read overlaps ignored, was 50.78 for LT1, 410.67□551.11 for UQ isolates, 88.35□92.70 for UT isolates, and 75.30 for JA1-1. Mean mapping quality was 58.99 for LT1, 58.95□59.07 for UQ isolates, 59.32□59.34 for UT isolates, and 59.3274 for JA1-1. High-quality reads were mapped against the NCBI reference genome assembly ASM148472v1 (GenBank CP012395.1) for *C. autoethanogenum* DSM 10061 (Humphreys et al., 2015). Two mutations were excluded from further analysis as they were considered non-relevant: one mutation was present in all isolates and the starting strain JA1-1, and one mutation was present in JA1-1 only.

Additionally, for LT1, the Illumina data was used to polish the PacBio genome assembly with the Pilon v1.24 tool (Walker et al., 2014). The polished assembly was deemed to be highly accurate based on the observation that no 100% frequency variants were predicted by breseq v0.35.1 (Deatherage and Barrick, 2014) using the polished assembly and Illumina data as inputs. The validated LT1 assembly was then deposited to the NCBI genome submission portal (Genbank CP110420) for annotation with the NCBI Prokaryotic Genome Annotation Pipeline.

2.7. Transcriptome analysis of UT isolate bioreactor chemostat cultures

Transcriptome analysis for the steady-state chemostat cultures of UT isolates listed in Table 1 was carried out using RNA sequencing (RNA-seq). In addition, the transcriptome of the non-steady-state culture of UT2 at D = 1 day^{-1} without apparent “CO toxicity” (end of culture in Supplementary Fig. 2; see text below for details) was also determined. This enabled the comparison of the transcriptome of the “CO toxicity” steady-state culture of UT2 at D = 1 day^{-1} with a “non-CO toxicity” culture at the same D.

Ten millilitres of culture were pelleted by centrifugation (5,000 × *g* for 3 min at 4ºC) and resuspended in 5 mL of RNAlater (76106; Qiagen). Samples were stored at 4ºC overnight, centrifuged (4,000 × *g* for 10min at 4ºC), and pellets stored at -80ºC until RNA extraction. Thawed pellets were resuspended in RLT buffer (74104; Qiagen) containing β-mercaptoethanol and lysed with acid-washed glass beads (G4649; Merck) using the Precellys® 24 instrument with liquid nitrogen cooling (Bertin Technologies). Total RNA was extracted using the RNeasy mini kit (74104, Qiagen) with off-

column TURBO™ DNase treatment (AM2239; Invitrogen), followed by purification and enrichment using the RNA Clean and Concentrator™ kit (R1018, Zymo). The efficiency of the total RNA purification and DNA removal was verified using the NanoDrop™ 1000 instrument (Thermo Scientific) and the quality of RNA extracts was checked using the TapeStation 2200 equipment (Agilent Technologies). Total RNA concentration was determined using the Qubit 2.0 instrument (Q32866; Invitrogen). Next, ribosomal RNA (rRNA) was removed using the QIAseq FastSelect – 5S/16S/23S Kit (335925; Qiagen) and stranded mRNA libraries were prepared using the QIAseq Stranded RNA Lib Kit (180743; Qiagen). RNA sequencing was performed using the NextSeq MID150 sequencing kit (20024904; Illumina) on the NextSeq500 sequencer (Ilumina) with 2 x 75 bp paired-end dual indexed (2 x 8 bp) reads.

The quality of raw NextSeq reads was verified using MultiQC (Ewels et al., 2016) and adapter sequences were trimmed using the Cutadapt Python package (version 2.10; Martin, 2011) allowing a minimum read length of 35 nt. The resulting high-quality paired-end reads were mapped to the NCBI reference genome assembly ASM148472v1 (GenBank CP012395.1) for *C. autoethanogenum* DSM 10061 (Humphreys et al., 2015) using the align function within Rsubread package (version 2.4.2; Liao et al., 2019). Then, four .bam files per sample were merged using Samtools (version 1.10; Li et al., 2009) and genomic features were assigned using the featureCounts functions within Rsubread. Transcript abundances were determined as described before (Valgepea et al., 2017a). Genes were determined to be differentially expressed by fold-change > 1.5 and q-value < 0.05 after false discovery rate correction (Benjamini and Hochberg, 1995) (Supplementary Table 1). RNA-seq data has been deposited in the NCBI Gene Expression Omnibus repository under accession number GSEXXX.

3. RESULTS

3.1. Autotrophic adaptive laboratory evolution (ALE) of *Clostridium autoethanogenum* JA1-1 for improved growth phenotypes

To improve growth phenotypes of the wild-type *Clostridium autoethanogenum* JA1-1 strain, three different autotrophic ALE strategies were employed across three facilities (Fig. 1a; see Materials and Methods for details). For the ALE experiment done at The University of Tartu (UT ALE), serial propagation of batch bottle cultures was employed for 142 generations with a gradual removal of YE at the start. For the ALE experiment done at The University of Queensland (UQ ALE), firstly serial propagation of batch cultures in serum bottles for 107 generations was used with a gradual removal of YE at the start. After that, the evolved population was transferred into a continuous bioreactor culture where it was grown for another 109 generations without YE. And for the third ALE

experiment done at LanzaTech, Inc. (LT ALE), cells from a bottle culture were exposed to the chemical mutagen NTG after which the culture was transferred into a continuous bioreactor culture and grown without YE for ~50 days. The UT ALE experiment was carried out on CO while the LT and UQ ALE experiments were done on syngas (CO, CO_2, H_2).

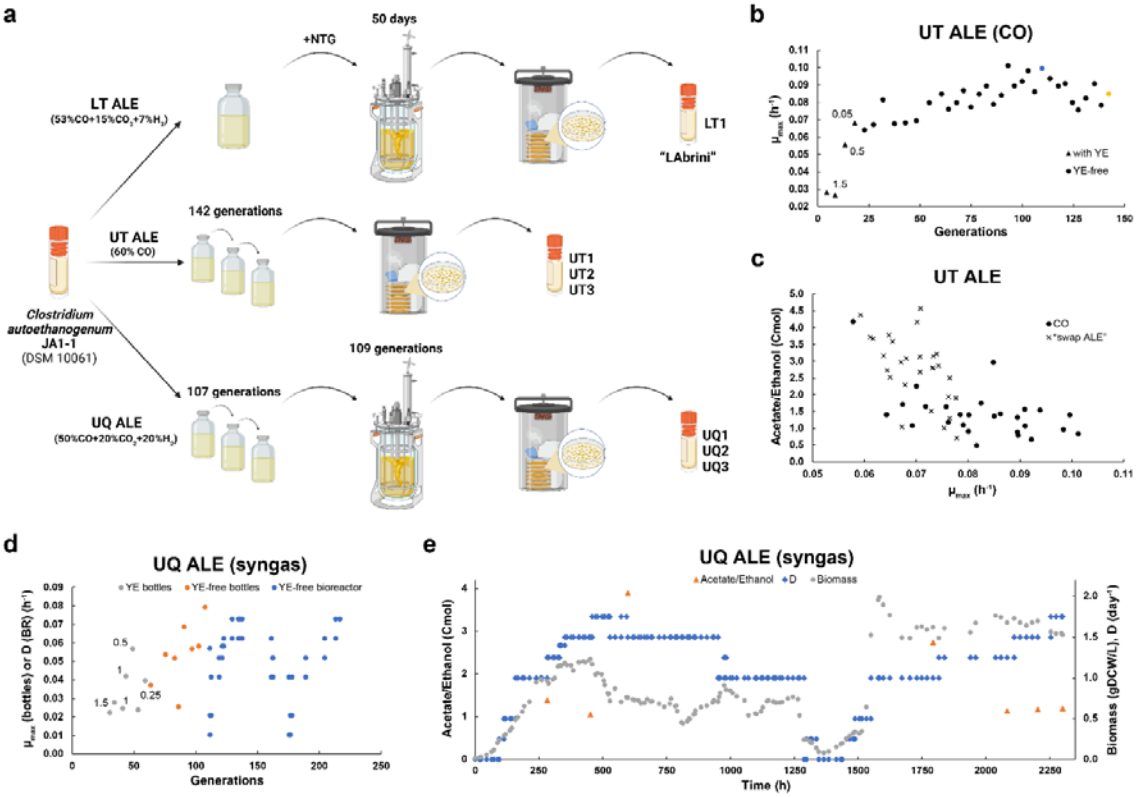

Fig. 1. Autotrophic adaptive laboratory evolution (ALE) of *Clostridium autoethanogenum* JA1-1 for improved growth phenotypes executed with three different approaches across three facilities. (a) Overview of the different ALE strategies employed. See text for details. Created with BioRender.com. (b) Change of maximum specific growth rate (μ_{max}) with batch culture generations during UT ALE on CO. Blue and yellow circles denote cultures that were used for isolating single colonies (see text for details). For cultures with generations ~43, ~48, ~96, and ~105, μ_{max} was calculated using two data points from the exponential phase instead of using 3⍰5 data points as for the rest. (c) Change of acetate/ethanol (Cmol) with μ_{max} in combined batch data from UT (UT ALE and UT "swap ALE"; see text for details). (d) Change of μ_{max} in batch or dilution rate (D) in bioreactor (BR) continuous cultures with culture generations during UQ ALE on syngas. (e) Change of acetate/ethanol, biomass concentration (biomass), and D over fermentation time during the continuous culture of UQ ALE on syngas. Numbers next to triangles (panel b) or circles (panel d) denote yeast extract (YE) concentrations. gDCW, gram of dry cell weight.

In UT ALE, serial propagation of CO bottle cultures allowed the YE in the media to be removed step-wise by the fourth subculture (Fig. 1b). Notably, a sudden ~2-fold increase of μ_{max} was observed during YE removal for the third sub-culture (first bottle with reduced YE, 0.5 g/L). The population reached its peak μ_{max} of 0.10 h^{-1} (~4.6-fold higher compared to start) by the ~93rd generation after

which a declining μ_{max} trend was observed. This phenomenon has been observed previously when carrying out ALE under constant conditions (LaCroix et al., 2015; Wiser et al., 2013). We also tested if higher μ_{max} values could be reached when transferring the ALE culture between CO and syngas ("UT swap ALE"), but this did not occur (Supplementary Fig. 1). Intriguingly, combined data from UT (UT ALE and "UT swap ALE") revealed a declining trend of the acetate/ethanol ratio with faster growth (Fig. 1c).

In UQ ALE, the experiment was started with four fructose batch cultures and then transferred to syngas bottles with step-wise removal of YE (Fig. 1d). The increase of μ_{max} during YE removal was not as abrupt as in UT ALE but the increasing trend was clear and the final batch bottle culture with ~107 generations reached a μ_{max} of 0.08 h^{-1} (~3.2-fold higher compared to first syngas bottle). Then, the evolved population was transferred to a chemostat bioreactor system where additional selective pressure was applied by changing the dilution rate (D; i.e. μ under steady-state) for ~109 generations. We obtained a stable culture at high biomass concentrations and D = 1.8 day^{-1} (μ = 0.08 h^{-1}) and the UQ ALE bioreactor culture seemed to excrete less acetate compared to ethanol with faster growth above D = 1 day^{-1} (Fig. 1e).

In LT ALE, *C. autoethanogenum* was first treated with the chemical mutagen NTG during growth with YE after which the culture was used to inoculate a continuous bioreactor culture to a final D of 1 day^{-1} without YE for ~50 days (Fig. 1a). For all the three ALE strategies, ALEs were terminated once significant changes in evolving population phenotypes were no longer observed (e.g. μ_{max} and maximum biomass in bottle cultures, gas data in continuous cultures).

3.2. Isolated ALE clones exhibit enhanced growth characteristics and metabolite production patterns

Next, we plated the evolved mixed populations to isolate single clones for detailed characterisation and for evaluating the level of phenotypic heterogeneity within the mixed populations. For UT ALE, we isolated clones from both the culture with peak μ_{max} of ~0.10 (blue marker in Fig. 1b) and the last ALE bottle with lower μ_{max} (yellow marker in Fig. 1b). Ten colonies were isolated for both UT and UQ ALE, respectively, for preliminary comparison of growth and by-product patterns in batch cultures with the same gas and media as in ALE. Notably, all isolates could be grown without the presence of YE, thus fulfilling the first aim of our work. For UT ALE, we expected that isolates from the peak μ_{max} population (blue marker) would grow faster than isolates from the last slower growing population (yellow marker): this was not, however, observed (Supplementary Fig. 3a). Variability in μ_{max} of UQ ALE isolate batch cultures was also seen (Supplementary Fig. 3b). Similarly, phenotypic heterogeneity in terms of by-product patterns within isolates of both UT and UQ ALE was observed (Supplementary Fig. 3c-d). In particular, some isolates of UT ALE showed lower acetate/ethanol

ratios while three isolates from UQ ALE with high ethanol production were detected. As a result, three isolates from both UT (UT1, UT2, UT3) and UQ ALE (UQ1, UQ2, UQ3) were selected for further detailed characterisation based on μ_{max} and intriguing metabolite production patterns in the preliminary screen (indicated with asterisks on Supplementary Fig. 3). From LT ALE, one isolate termed LT1 was selected for further study.

We grew the seven selected isolates in autotrophic batch bottle cultures without YE with frequent sampling to more accurately compare growth and by-product patterns. UT and UQ ALE isolates were grown on the gas they were evolved on, CO and syngas, respectively; the isolate obtained through chemical mutagenesis – LT1 – was grown on both. For comparison, the starting wild-type strain for all ALE strategies – *C. autoethanogenum* JA1-1 – was also cultured on both gases but with YE supplementation as we could not observe growth on CO without YE after 520 h. During growth on CO, isolate UT3 had the highest μ_{max} (0.08 h^{-1}) among UT ALE while the fastest growth on CO was shown by LT1 with a μ_{max} of 0.10 h^{-1} (Fig. 2a). In comparison, the starting ALE strain JA1-1 showed a μ_{max} of 0.02 h^{-1} (with YE) that is ~2- to ~4-fold lower than all the evolved isolates tested on CO. During growth on syngas, UQ1, UQ3, and LT1 showed similar growth (μ_{max} ~0.08 h^{-1}) that was ~1.3- and ~3-fold higher than for UQ2 and JA1-1 (with YE), respectively (Fig. 2b). All evolved isolates grew faster than the starting strain, thus fulfilling the second aim of our work of obtaining faster-growing strains.

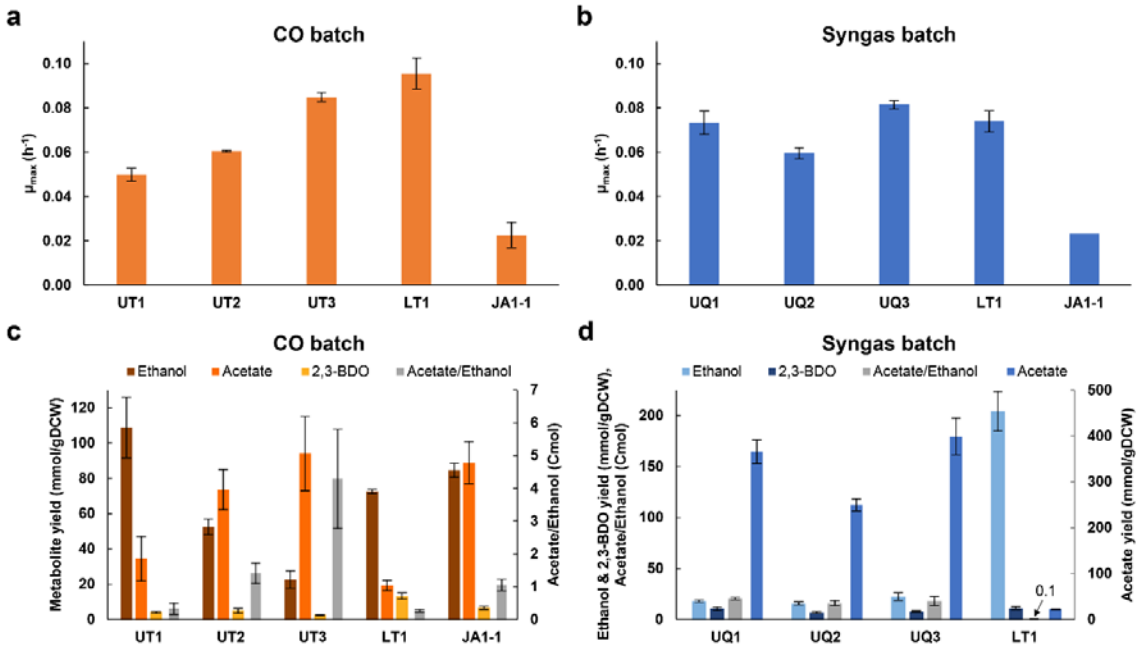

Fig. 2. Autotrophic characterisation of selected isolates from UT, UQ, and LT ALE, and the wild-type *C. autoethanogenum* starting strain of ALE (JA1-1) in batch cultures. (a) Maximum specific growth rate (μ_{max}) of UT and LT ALE isolates and JA1-1 in CO batch cultures. (b) μ_{max} of UQ and LT ALE isolates and JA1-1 in syngas batch cultures. (c) Production yields

(mmol/gDCW) of growth by-products and acetate/ethanol (Cmol) of UT and LT ALE isolates and JA1-1 in CO batch cultures. (d) Production yields (mmol/gDCW) of growth by-products and acetate/ethanol of UQ and LT ALE clones and JA1-1 in syngas batch cultures. All data for UT, UQ, and LT isolates are from yeast extract (YE)-free medium, JA1-1 data are from medium with YE. Data are average ± standard deviation between bioreplicates (see Material and Methods for details). gDCW, gram of dry cell weight; 2,3-BDO, 2,3-butanediol.

Frequent sampling also enabled us to accurately determine production yields (mmol/gDCW) for the detected growth by-products acetate, ethanol, and 2,3-BDO. Notably, the lowest acetate/ethanol ratios were detected on CO for isolates LT1 (0.27) and UT1 (0.32) that were ~4- and ~3-fold lower than for JA1-1 (1.05) (Fig. 2c). While UT1 showed the highest ethanol production yield with the lowest μ_{max} of the evolved strains, the fastest growing UT ALE isolate UT3 showed the highest acetate production yield and acetate/ethanol of 4.14 (Fig. 2a and c). The production yield of 2,3-BDO was the highest for LT1, making the strain overall the most favourable on CO in terms of reduced by-products (Fig. 2c). Importantly, LT1 demonstrated preferable metabolite production also during growth on syngas in comparison with UQ isolates (Fig. 2d): it showed a >6-fold higher ethanol production yield with the lowest acetate production yield, translating into a low acetate/ethanol ratio of 0.70. The highest 2,3-BDO production yields were shown by UQ1 and LT1. Interestingly, higher acetate production yields for UT and UQ isolates correlate well with higher μ_{max} while LT1 achieves fast growth with significantly lower acetate production (Supplementary Fig. 4). These extracellular metabolomics data support the notion that evolving acetogens in the presence of C1 gases trigger rearrangements in central carbon metabolism (Tremblay et al., 2015).

3.3. Bioreactor continuous gas fermentation cultures show the superiority of isolate LT1

We next tested the performance and robustness of all UT ALE isolates, LT1, and UQ1 in continuous gas fermentation bioreactor as this is the industrially relevant condition (Köpke and Simpson, 2020). Steady-state continuous cultures also provide the necessary data to describe the physiological state of the cell (e.g. μ, gas uptake, by-products, carbon distribution) (Adamberg et al., 2015). In total, 25 steady-states were achieved across chemostat cultures for strains grown either on CO or syngas at D ranging from ~0.5 to ~2 day^{-1} (D = μ at steady-state) (Table 1).

Table 1. Summary of 25 steady state chemostat cultures of UT, LT1, and UQ1 isolates.

Isolate	Feed gas	Gas flow rate (mL/min)	Agitation (RPM)	D (day^{-1})	Biomass concentration (gDCW/L)	Number of replicates
UT2	CO	35	690	1.00 ± 0.00	0.52 ± 0.03	3
UT3*	CO	28	570	0.49 ± 0.01	1.03 ± 0.15	3

UT1	CO	28	570	0.53 ± 0.00	1.13 ± 0.06	3
UT2	CO	24	570	0.52 ± 0.01	0.88 ± 0.09	4
LT1	Syngas	50	675	0.99 ± 0.04	1.41 ± 0.09	4
LT1	Syngas	72	800	1.97 ± 0.11	1.50 ± 0.07	4
LT1	Syngas	35	525	0.50 ± 0.06	0.42 ± 0.05	2
UQ1	Syngas	35	525	0.50 ± 0.06	0.42 ± 0.05	2

D, dilution rate; gDCW, gram of dry cell weight. Data are average ± standard deviation between bioreplicates. Syngas composition - 50% CO, 20% CO_2, 20% H_2, 10% Ar; *steady-state reached only for gas uptake and production rates.

We initially aimed to run all strains at D = 1 day^{-1}, but failed after multiple attempts to obtain steady-state at D = 1 day^{-1} on CO for UT2 at CO uptake rates (COUR) of ~1200 mmol/L/day and biomass concentrations of ~1.5 gDCW/L. We did obtain steady-state at D = 1 day^{-1} for UT2 at COUR ~400 mmol/L/day and interestingly CO uptake could only be increased after strongly decreasing the CO% in the bioreactor headspace through changing gas-liquid mass transfer (Supplementary Fig. 2; between ~380 to ~440 h), but no steady-state was obtained. Thus UT2 might have struggled due to CO toxicity. For this "CO toxicity" steady-state of UT2 at D = 1 day^{-1} (Table 1; up to ~380 h on Supplementary Fig. 2), transcriptome analysis revealed a starkly different transcriptional profile compared to all other cultures (Supplementary Fig. 5). The transcriptional profile was also very distinct from the unstable "non-CO toxicity" phase of the same culture operated at same D (from ~480 h on Supplementary Fig. 1. Notably, we detected strong up-regulation of numerous hypothetical, putative membrane, and sporulation-related proteins and down-regulation of the HytA-E/FdhA complex components (Supplementary Table 1). After these challenges with UT2 cultures and challenges in gas uptake with UQ1 at D = 1 day^{-1}, we decided to use D = 0.5 day^{-1} to compare strains across gases.

For UT3 though, we could obtain steady-state data at D = 0.5 day^{-1} only in terms of gas uptake and production since acetate and ethanol production were highly sensitive to any operational activities to the culture (e.g. halting agitation for a volume check, sampling 1% of culture volume). Furthermore, adjustment of gas-liquid mass transfer was needed even after obtaining target agitation and gas flow (Fig. 3). In striking comparison, operating LT1 cultures was straightforward and thus we additionally achieved steady-states at D = 1 and 2 day^{-1} at high COUR and biomass concentrations (Fig. 3). The COUR for LT1 growing on syngas at D = 1 day^{-1} is triple of the steady-state value of UT2 on CO (Supplementary Fig. 6). Moreover, faster gas-liquid mass transfer ramping and higher Ds also meant that two steady-states were achieved for LT1 with half the time it took to achieve one steady-state for UT3 (Fig. 3). The robustness of LT1 is highly relevant for the academic community as it makes it significantly less challenging to operate continuous gas fermentation

cultures to obtain high-quality data. Thus a robust strain for bioreactor continuous gas fermentation was obtained that fulfils the third aim of our work.

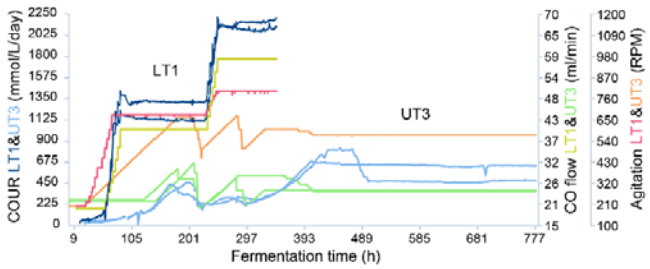

Fig. 3. Robustness of strain LT1 in terms of operation of bioreactor continuous gas fermentation cultures. LT1 data are for the chemostats that achieved steady-states at specific growth rates (μ) of 1 and 2 day^{-1}. See Table 1 for more details on LT1 and UT3 chemostats. COUR, CO uptake rate (mmol/L/day); RPM, rounds per minute.

A comparison of steady-state data from the bioreactor runs demonstrates that various metabolic rearrangements took place during the three ALE strategies (Fig. 4). Different from the batch data (Fig. 2), UT strains showed similar growth characteristics in CO chemostats (D = 0.5 day^{-1}) with the exception of 2,3-BDO production (Fig. 4). While the acetate concentration for UT2 was lower most likely due to lower biomass concentration (Fig. 4a), specific by-product production rates (Fig. 4b) and specific gas rates (Fig. 4c) showed similar values, except for the specific production rate of 2,3-BDO ($q_{2,3\text{-BDO}}$; mmol/gDCW/day). Chemostat results were different from batch data also when comparing UQ1 and LT1 in syngas chemostats at D = 0.5 day^{-1} (Fig. 4). The two strains showed very similar performance at the same D both in terms of by-product production and gas uptake and production. Notably, LT1 outperformed all strains with regard to acetate/ethanol ratios by showing values <1 at D = 1 and 2 day^{-1} (Fig. 4a). The ability to achieve higher biomass concentrations for LT1 D = 1 and 2 day^{-1} cultures also translated into the highest ethanol and 2,3-BDO levels (Fig. 4a) and due to faster growth also to higher specific production rates (q_{EtOH} and $q_{2,3\text{-BDO}}$) (Fig. 4b). LT1 cultures at D = 1 and 2 day^{-1} also show the highest carbon flux to the reduced ethanol and 2,3-BDO products across the various strains and steady-states (Fig. 5). Similarly to the latter strain, the specific H_2 uptake rate (q_{H2}) for LT1 did not increase proportionally with D (Fig. 4c), suggesting another avenue for improving *C. autoethanogenum* performance through ALE, i.e. improving H_2 uptake.

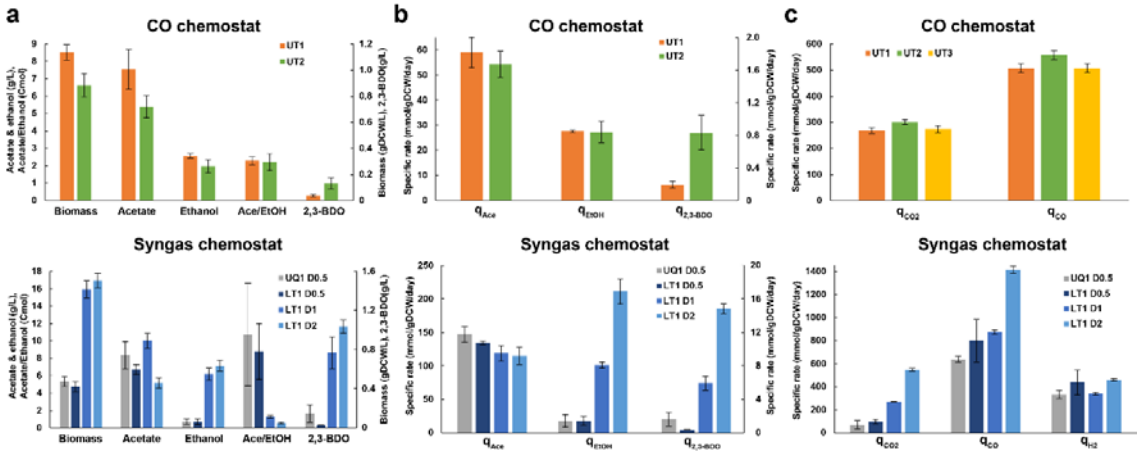

Fig. 4. Characterisation of selected isolates from UT, UQ, and LT ALE in autotrophic chemostat cultures. (a) Biomass and by-product concentrations and acetate/ethanol (Ace/EtOH). (b) Specific by-product production rates (mmol/gDCW/day). (c) Specific gas uptake (CO, H_2) and production (CO_2) rates. CO chemostat data for UT1 and UT2 are from dilution rate (D) 0.5 day^{-1}; for syngas chemostat data, number following D denotes D value in day^{-1}. UT3 reached steady-state only regarding gas uptake and production. Data are average ± standard deviation between bioreplicates (see Table 1). See Table 1 for details. gDCW, gram of dry cell weight; 2,3-BDO, 2,3-butanediol; q, specific rate.

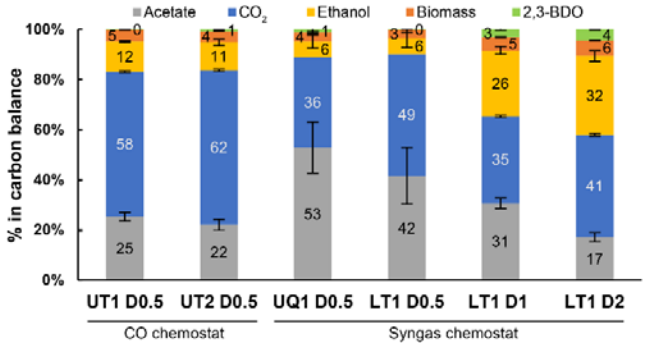

Fig. 5. Carbon balances of selected isolates from UT, UQ, and LT ALE in autotrophic chemostat cultures. Number following D (dilution rate) denotes D value in day^{-1}. Carbon flow into CO_2 for UQ1 D0.5 and LT1 D0.5 were calculated based on measured carbon flows into other products and biomass by assuming 100% carbon recovery. Carbon recoveries for UT and LT D1 and D2 were normalised to 100% to have a fair comparison of carbon distributions between different conditions. Data are average ± standard deviation between bioreplicates (see Table 1). See Table 1 for details. 2,3-BDO, 2,3-butanediol.

The evolved strain LT1 fulfilled all the aims of our work to create an improved model-acetogen strain for the community: it grows without complex nutrients on minimal medium, shows high gas uptake enabling faster growth, and is robust in terms of operating continuous bioreactor gas fermentation cultures. Additionally, the metabolic feature of high carbon flux into reduced growth by-products makes LT1 an attractive chassis for metabolic engineering. We have thus deposited the LT1 strain at the DSMZ strain collection (DSMX) for community use and propose to make it the

model-acetogen strain named *C. autoethanogenum* LAbrini (i.e. Laboratory Adapted Abrini). The improved characteristics of LAbrini hold promise for speeding up both phenotyping and engineering of acetogens. For example, we are currently mapping genotype-phenotype links for every gene in LAbrini using a systems-level approach (ARC, 2021).

3.4. Genetic mutations associated with improved phenotypes

We next used whole-genome DNA sequencing (WGS) to identify genetic mutations that took place during the three ALE strategies and may have led to different phenotypes. WGS data also allow to compare genetic variability between the evolved strains. We sequenced the starting strain JA1-1 and seven key evolved strains (UT1, UT2, UT3, UQ1, UQ2, UQ3, and LT1) and performed mutation analysis after high-quality genome assemblies (see Material and Methods). The starting strain for our three ALE strategies was sequenced to ensure that we reliably detect genetic mutations that appeared during ALE instead of only relying on the published genome sequences for *C. autoethanogenum* JA1-1 (Brown et al., 2014; Humphreys et al., 2015).

Principal component analysis (PCA) of all the WGS data revealed that the majority of variability across the eight sequences is explained by PC1 (65.6%) and PC2 (24.5%) (Fig. 6a; Supplementary Fig. 7). Importantly, PCA also illustrated clear separation of WGS data between the three ALE strategies – UT ALE strains obtained through serial propagation of batch cultures clustered very close (and closest to the starting strain) while UQ ALE strains obtained from a continuous culture after serial propagation of batch cultures showed higher variability (Fig. 6a). The LT1 strain obtained through chemical mutagenesis and with superior bioreactor performance was positioned between the UT and UQ ALE strains. The genome of LT1 is 4,349,910 nt long, contains 3,942 protein coding sequences (CDSs), and has a GC content of 31.1%. These values are similar but not identical to JA1-1 due to a large genomic deletion and a different annotation LT1 (values for JA1-1 are as follows: 4,352,446 nt long; 3,964 CDSs; 31.1% GC content).

In total, 25 mutations were detected across the seven evolved strains with 21 of them affecting CDSs (Fig. 6b and c; Supplementary Table 2). 17 of the 25 mutations were single nucleotide polymorphisms (SNPs) and eight were deletions, while four being ≥ 168 bp (Fig. 6c). Two hot-spots were detected in the genome that accrued mutations during multiple ALE strategies: mutations #19–23 around genome position 3,803,000 (all in the same CDS) and mutations #4–5 around position 883,000 (both in the same CDS (Fig. 6b and c). This points towards regions and genes under stronger evolutionary pressure.

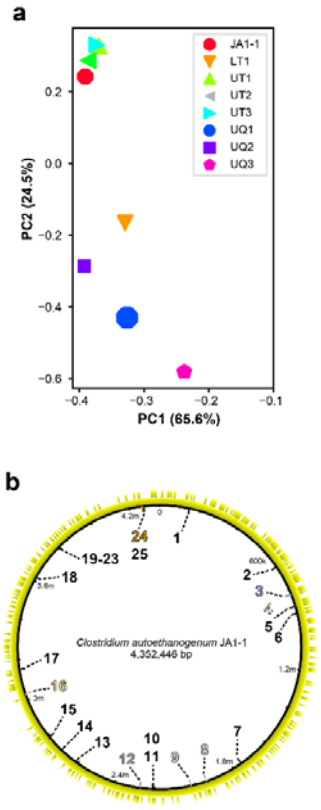

c

Strain	Mut. #	Position	Mutation	FC	Gene ID	Description of protein product
LT1	1.	146,518	Δ2,717 bp	CDS	CLAU_3832-3830	Pyrimidine-nucleoside phosphorylase (3832); phosphopentomutase (3831); nucleoside transporter domain protein (3830)
	5.	883,401	G→T	CDS	CLAU_3129	Sporulation transcriptional activator Spo0A
	13.	2,608,385	G→T	CDS	CLAU_1579	Carbon-monoxide dehydrogenase (acceptor)
	14.	2,700,831	G→T	CDS	CLAU_1506	Ribonuclease PH
	25.	4,270,741	T→C	NC		
UT1	3.	819,259	G→A	CDS	CLAU_3194	Histidine kinase
	9.	2,018,506	C→A	NC		
	10.	2,201,466	G→A	CDS	CLAU_1957	Two component transcriptional regulator winged helix family
	16.	3,029,158	A→G	NC		
	19.	3,802,766	Δ231 bp	CDS	CLAU_0471	Amino acid permease
UT2	3.					
	9.					
	11.	2,205,563	(A)9→8	CDS	CLAU_1953	Transcription-repair coupling factor
	16.					
	23.	3,804,103	G→T	CDS	CLAU_0471	Amino acid permease
UT3	3.					
	7.	1,746,635	C→T	CDS	CLAU_2375	Putative signal transduction protein with CBS and DRTGG domain-containing protein
	9.					
	16.					
	21.	3,803,557	Δ527 bp	CDS	CLAU_0471	Amino acid permease
UQ1	4.	882,681	G→T	CDS	CLAU_3129	Sporulation transcriptional activator Spo0A
	6.	925,342	Δ168 bp	CDS	CLAU_3080-3079	Pseudouridine synthase (3080); lipoprotein signal peptidase (3079)
	12.	2,268,926	(CAGCAC) 2→1	CDS	CLAU_1904	Ribosomal protein S12
	15.	2,786,811	C→A	CDS	CLAU_1423	Ferric uptake regulator Fur family
	17.	3,151,872	C→A	CDS	CLAU_1076	Cobalamin synthesis protein cbiG
	18.	3,618,615	(18-bp) 5→2	CDS	CLAU_0649	Putative secreted protein containing bacterial Ig-like domain
	22.	3,803,844	T→G	CDS	CLAU_0471	Amino acid permease
	24.	4,265,493	(A)8→7	NC		
UQ2	4.					
	8.	1,937,991	A→G	CDS	CLAU_2202	Transcriptional regulator AbrB family
	12.					
	22.					
	24.					
UQ3	2.	668,458	C→A	CDS	CLAU_3345	Methyl-accepting chemotaxis protein
	4.					
	8.					
	12.					
	20.	3,803,210	G→A	CDS	CLAU_0471	Amino acid permease
	24.					

Fig. 6. Whole-genome sequencing of the selected isolates from UT, UQ, and LT ALE and identified mutations relative to the wild-type *C. autoethanogenum* starting strain of ALE (JA1-1). (a) Principal component analysis (PCA) of sequence variability between the 7 strains. (b) Distribution of the identified 25 mutations across the circular genome of JA1-1. Number denotes mutation shown in panel c (column Mut. #) and colour matches shading of mutation in panel c (exceptions are numbers in black that have white shading in panel c). Yellow layers are protein coding sequences (CDS) on forward (inner) and reverse (outer) strands. (c) Details of the 25 mutations identified in the 7 ALE strains. Mutations with colour shading denote mutations identified in more than one strain (details shown only for the first occurrence); shading colours match colour of numbers (Mut. #) on panel b. The bases within the parentheses in column "Mutation" denote the repeat sequence that was decreased from the number of repeats indicated on the left of the arrow (→) to the number indicated on the right of the arrow. See Supplementary Table 2 for additional details on mutations. PC, principal component; Mut #, mutation number; FC, feature class; Gene ID, gene identifier; SNP, single nucleotide polymorphism; Δ, deletion; NC, non-coding.

The first hot-spot at ~3,803,000 position is a proposed amino acid permease (CLAU_0471; function predicted based on conserved domain PotE) that was affected by two deletions and three different SNPs: one 231 bp deletion in UT1 and one 527 bp deletion in UT3; two hits in UQ isolates and one in UT2 (mutations #19–23 in Fig. 6c and Supplementary Table 2). Interestingly, nucleotides in the ALE starting strain JA1-1 at these three SNP positions of CLAU_0471 are fully conserved across homologs of Clostridia species (Supplementary Fig. 8). The second hot-spot at position ~883,000 is the sporulation transcription factor *spo0A* (CLAU_3129) that was affected by a C-to-A SNP at two

different locations in UQ and LT ALE (mutations #4–5 in Fig. 6c and Supplementary Table 2). Similarly to mutations in the first hot-spot (Supplementary Fig. 8), nucleotides in the starting strain JA1-1 at both positions of the second hot-spot are highly conserved across homologs of Clostridia species (Supplementary Fig. 9). UQ1 acquired a 168 bp deletion (mutation #6) across genes encoding for a lipoprotein signal peptidase (CLAU_3079) and a pseudouridine synthase (CLAU_3080) that are involved in sporulation (Fimlaid et al., 2015) and pyrimidine metabolism, respectively (Fig. 6c and Supplementary Table 2). Interestingly, the latter gene was upregulated under butanol stress in a *spo0A* overexpression mutant strain in *Clostridium acetobutylicum* (Alsaker et al., 2004). Pyrimidine metabolism seems to have played an important role for improving strain phenotypes in our ALE approaches as the large 2,717 bp deletion in LT1 (mutation #1) resulted in deletion of two genes (CLAU_3830 and 3831) and truncation of one gene (CLAU_3832) that are associated with pyrimidine metabolism (Fig. 6c and Supplementary Table 2).

Among the other spatially dispersed mutations in the genome, the mutation potentially most relevant to the improved phenotype of LT1 is a SNP (mutation #13) in the carbon monoxide dehydrogenase gene AcsA (CLAU_1579) that encodes for the CODH subunit of the CODH/acetyl-CoA synthase (ACS) protein complex (Fig. 6c and Supplementary Table 2). Mutation #13 removes the AcsA stop codon and results in a putative translational fusion product. The only CDS mutation (#3) present in all UT ALE strains was found in a predicted histidine kinase (CLAU_3194), which is interesting as some histidine kinases regulate sporulation and metabolism in Clostridia (Xin et al., 2020). Notably, one SNP appeared during UQ ALE in a normally highly conserved position in Clostridia species (Supplementary Fig. 10) - mutation #8 in an AbrB family transcriptional regulator (CLAU_2202) (Fig. 6c and Supplementary Table 2). Interestingly, CLAU_2202 is among the top 100 abundant proteins in *C. autoethanogenum* (Valgepea et al., 2022). Other potentially relevant mutations in CDSs appeared in a ribosomal protein S12 (mutation #12), and transcription-associated genes (mutations #10, #11, and #15). Future advances in the quantification of genotype-to-phenotype links in acetogens will assist in interpreting the genetic changes we detected and improve experimental evidence-based (vs. computationally derived) annotation of *C. autoethanogenum* genome.

4. DISCUSSION

While gas fermentation using *C. autoethanogenum* has been deployed at commercial scale for ethanol production (Köpke and Simpson, 2020), non-commercial acetogen strains struggle to grow on minimal medium, show slow gas uptake and growth, and are challenging to run in continuous bioreactor cultures. To overcome these limitations, we used a comprehensive ALE approach in this work to provide the academic community with a public strain LAbrini (LT1) with superior

performance in acetogen gas fermentation. We characterised the evolved strains using bottle and bioreactor cultures, gas analysis, metabolomics, transcriptomics, and DNA sequencing.

During one of the ALEs (UT), we noticed a declining μ_{max} during the last ⅓ of the ALE (Fig. 1b). This implies that evolutionary pressures other than towards growing faster were involved in this ALE approach of serial batch culture propagation. Similar trends have been seen before (LaCroix et al., 2015; Wiser et al., 2013). Additionally, UT ALE populations showed a declining trend of acetate/ethanol with faster growth (Fig. 1c). Some isolates of the ALE populations of this work displayed faster growth coupled with higher acetate production (Supplementary Fig. 4). These opposing observations at isolate and population levels suggest that cells can find various metabolic routes across different ALE approaches to achieve faster growth, as noted before (Barrick et al., 2009; Fong et al., 2005). We hypothesise that cross-feeding between subpopulations took place similar to previous bacterial ALEs (Good et al., 2017; Helling et al., 1987; Rozen and Lenski, 2000; Treves et al., 1998). Future co-culturing experiments of isolates with different phenotypes (e.g. high and low acetate producers) might shed light on these possibilities.

Characterisation of evolved strains in both batch and chemostat cultures revealed that batch bottle cultures might fail to predict performance in continuous cultures. For example, UT1 and UT2 showed nearly identical q_{EtOH} and acetate/ethanol ratios in chemostats after very dissimilar results in batch cultures and only LT1 was able to grow robustly above D = 0.5 day^{-1} while most evolved strains showed similar μ_{max} in batch cultures, which was >0.5 day^{-1}. Furthermore, efforts to operate UT1 chemostats at higher D and gas-liquid mass transfer seemed to have been compromised by CO toxicity (see below), which was not present in batch cultures with lower gas-liquid mass transfer. These results emphasise the importance of testing novel strains (e.g. acquired using ALE or metabolic engineering) in industrially-relevant continuous fermentation conditions (Köpke and Simpson, 2020).

Transcriptome analysis of the potential "CO toxicity" state of UT1 chemostat at D = 1 day^{-1} revealed a very distinct transcriptional profile compared to other cultures, including UT1 in a "non-CO toxicity" but unstable culture at D = 1 day^{-1}. UT1 in the "CO toxicity" state showed strong up-regulation of numerous hypothetical and sporulation-related proteins (Supplementary Table 1). These proteins serve as promising candidates for potential overexpression to play a role in mitigating CO toxicity. Intriguingly, we also observed ~2-fold down-regulation of components of the electron-bifurcating hydrogenase/formate dehydrogenase HytA-E/FdhA complex (Wang et al., 2013), which plays a key role in CO_2 reduction to formate in *C. autoethanogenum* using NADPH and reduced ferredoxin (Fd) or H_2 (Mock et al., 2015; Valgepea et al., 2017a; Wang et al., 2013). Wang and co-workers who purified the complex hypothesised that it might also play a role in protecting cells from

over-reduction of NADP and Fd pools during growth on CO (Wang et al., 2013). They propose that lowered CO oxidation (i.e. lower Fd reoxidation) increases the CO concentration in cells that inhibits CO_2 reduction to formate by the complex that further lowers reoxidation of Fd. The solution for avoiding this over-reduction state is NADPH and Fd reoxidation by HytA-E through proton reduction to H_2. Our results are consistent with their hypothesis as we detected H_2 production when trying to improve COUR of the UT1 "CO toxicity" culture by decreasing gas-liquid mass transfer, i.e. CO oxidation (Supplementary Fig. 2). We thus hypothesise that such regulation could be linked to the down-regulation of HytA-E/FdhA complex component genes. Metabolism of *C. autoethanogenum* thus displays reactional plasticity in choosing electron sinks to drive CO_2 reduction as proposed before (Lemaire et al., 2020; Wang et al., 2013). Such flexibility would realise growth advantages under changing environmental conditions.

Analysis of our ALE experimental data confirmed previous observations that different ALE approaches often lead to similarly improved phenotypes but through various underlying genetic changes (Barrick et al., 2009; Fong et al., 2005; Good et al., 2017; Helling et al., 1987; Treves et al., 1998). Genes that accumulate mutations across multiple ALEs are under stronger selection pressure and hence serve as attractive targets for further genetic engineering studies (Dragosits and Mattanovich, 2013). Interestingly, a proposed amino acid permease (CLAU_0471) was affected in all the isolated strains in two different ALE approaches (UT and UQ) by two distinct deletions and three SNPs. It is unclear why a proposed amino acid permease was under such strong selective pressure when the complex nutrient YE was removed from the medium. The other gene that was mutated during two of the ALEs (LT and UQ) was *spo0A* (CLAU_3129) which is a master regulator of sporulation and solventogenesis in Clostridia (Dürre, 2016; Kolek et al., 2017; Paredes et al., 2005; Steiner et al., 2011). Down-regulation or inactivation of *spo0A* in *C. acetobutylicum* causes a reduction in sporulation and increased solvent production (Harris et al., 2002; Li et al., 2016). Sporulation was likely further affected in UQ1 by the truncation of a lipoprotein signal peptidase (CLAU_3079), which is involved in sporulation of *Clostridium difficile* (Fimlaid et al., 2015). Interestingly, similar phenotypic changes could have been achieved in UT ALE through mutation #3 in a proposed histidine kinase (CLAU_3194) as similar kinases regulate sporulation and solventogenesis in *Clostridium beijerinckii* and *C. acetobutylicum* (Xin et al., 2020; Xu et al., 2015) and can directly interact with Spo0A (Paredes et al., 2005; Steiner et al., 2011). Sporulation could have been affected also during UQ ALE since the gene, pseudouridine synthase (CLAU_3080), that was deleted in UQ1 (mutation #6) was upregulated in a *spo0A* overexpression mutant strain in *C. acetobutylicum* (Alsaker et al., 2004). We hypothesise that mutations in above-described genes

could have emerged from selective pressure towards faster growth since suppression of sporulation functionalities would save cells valuable energy to grow faster.

The CODH/ACS complex realises both CO oxidation/CO_2 reduction and acetyl-CoA synthesis (Lemaire and Wagner, 2021), and its activity is essential for autotrophic growth of *C. autoethanogenum* (Liew et al., 2016). The removal of the *acsA* (CLAU_1579) stop codon in strain LT1 has been reported previously in an independent study that observed translational readthrough at the protein level (Liew et al., 2016). The *C. autoethanogenum* AcsA protein is uniquely truncated compared to other acetogens. The other potential key genetic modification in LT1 seems to be associated with pyrimidine metabolism evidenced by the large 2,717 bp deletion affecting three genes in pyrimidine metabolism. This could realise faster supply of RNA monomers that would in turn allow higher rates of translation and faster growth. Thus, the superior performance of LAbrini in continuous bioreactor cultures and its ability to grow in the absence of YE is due to its genotype and the selection strategy employed in its development. While growth without YE has been reported for acetogens before (Martin et al., 2015; Schulz et al., 2023), it is unclear if these phenotypes were the result of adaptation or evolution. Further studies are required to link mutations to its phenotype, key structural/functional attributes of the ACS/CODH enzyme complex and its regulation.

5. CONCLUSIONS

Our work is important for two reasons. First, we offer a superior model-acetogen strain – LAbrini – for the community that grows fast without complex nutrients, is robust for continuous gas fermentation cultures, and shows high carbon flux to reduced by-products. These strain characteristics will speed up both phenotyping and metabolic engineering of acetogens. Second, our comprehensive ALE approach with three different strategies offers important insights into convergent evolution trajectories in acetogens and highlights numerous novel engineering targets. Future work is needed to validate the causality of the mutations by reconstructing mutations of interest, both in combination and in isolation, and assaying their contribution to observed phenotypes. Future ALE experiments with LAbrini should potentially be designed to select for improved H_2 uptake, CO tolerance, and by-product tolerance.

DECLARATION OF INTEREST

LanzaTech has interest in commercial gas fermentation with *C. autoethanogenum*. AH, SB, GH, JD, LT, HZ, ROJ, VR, and MK are employees of LanzaTech.

ACKNOWLEDGEMENTS

This work was funded by the European Union's Horizon 2020 research and innovation programme under grant agreement N810755 and the Estonian Research Council's grant agreement PSG289. Australian Government funding through its investment agency, the Australian Research Council, towards the ARC Centre of Excellence in Synthetic Biology (CE200100029) is gratefully acknowledged. We thank Kristina Reinmets and Ugochi Jennifer Nwaokorie for valuable comments on the manuscript.

DATA AVAILABILITY STATEMENT

RNA sequencing data have been deposited in the NCBI Gene Expression Omnibus repository under accession number GSEXXX. The genome assembly of strain LT1 ("LAbrini") has been deposited to the NCBI genome submission portal with reference Genbank CP110420.

AUTHOR CONTRIBUTIONS

Conceptualization: HI, JKH, AH, EM, SB and KV; Methodology: HI, JKH, AH, SB, AYS, MJP, LAL, KRM, RAGG, GH, JD, LT, HZ, ROJ, VR, MK, EM, and KV; Formal analysis: HI, JKH, AYS, MJP, LAL, KRM, SB, VR, and KV; Investigation: HI, JKH, AH, SB, AYS, MJP, LAL, KRM, RAGG, GH, JD, LT, HZ, ROJ, and KV; Resources: SDS, MK, EM, and KV; Writing – Original Draft: HI and KV; Writing – Review & Editing: HI, JKH, AH, SB, AYS, MJP, LAL, KRM, RAGG, LT, HZ, ROJ, VR, SDS, MK, EM, and KV; Supervision: MK, EM, and KV; Project Administration: MK, EM, and KV; Funding Acquisition: SDS, MK, EM, and KV.

SUPPLEMENTARY MATERIAL CAPTIONS

Supplementary Figures. Supplementary Figures

Supplementary Table 1. Differentially expressed genes (DEGs) across different strains and conditions.

Supplementary Table 2. Additional details of the 25 mutations identified in the seven ALE strains.

REFERENCES

Abrini, J., Naveau, H., Nyns, E.-J., 1994. *Clostridium autoethanogenum*, sp. nov., an anaerobic bacterium that produces ethanol from carbon monoxide. Arch. Microbiol. 161, 345–351. https://doi.org/10.1007/bf00303591

Adamberg, K., Valgepea, K., Vilu, R., 2015. Advanced continuous cultivation methods for systems microbiology. Microbiol. 161, 1707–1719. https://doi.org/10.1099/mic.0.000146

Alsaker, K. V., Spitzer, T.R., Papoutsakis, E.T., 2004. Transcriptional Analysis of spo0A Overexpression in Clostridium acetobutylicum and Its Effect on the Cell's Response to Butanol Stress. J. Bacteriol. 186, 1959–1971. https://doi.org/10.1128/JB.186.7.1959-1971.2004

ARC, 2021. https://www.coesb.com.au/using-genes-to-improve-conversion-of-greenhouse-gases/

Barrick, J.E., Yu, D.S., Yoon, S.H., Jeong, H., Oh, T.K., Schneider, D., Lenski, R.E., Kim, J.F., 2009. Genome evolution and adaptation in a long-term experiment with *Escherichia coli*. Nature 461, 1243–1247. https://doi.org/10.1038/nature08480

Benjamini, Y., Hochberg, Y., 1995. Controlling the False Discovery Rate: A Practical and Powerful Approach to Multiple Testing. J. R. Stat. Soc. Ser. B 57, 289–300. https://doi.org/10.1111/J.2517-6161.1995.TB02031.X

Bourgade, B., Minton, N.P., Islam, M.A., 2021. Genetic and metabolic engineering challenges of C1-gas fermenting acetogenic chassis organisms. FEMS Microbiol. Rev. 45:fuab008. https://doi.org/10.1093/femsre/fuab008

Brown, S.D., Nagaraju, S., Utturkar, S., De Tissera, S., Segovia, S., Mitchell, W., Land, M.L., Dassanayake, A., Köpke, M., 2014. Comparison of single-molecule sequencing and hybrid approaches for finishing the genome of *Clostridium autoethanogenum* and analysis of CRISPR systems in industrial relevant Clostridia. Biotechnol. Biofuels 7:40. https://doi.org/10.1186/1754-6834-7-40

Deatherage, D.E., Barrick, J.E., 2014. Identification of Mutations in Laboratory-Evolved Microbes from Next-Generation Sequencing Data Using breseq, in: Methods in Molecular Biology (Clifton, N.J.). pp. 165–188. https://doi.org/10.1007/978-1-4939-0554-6_12

Dragosits, M., Mattanovich, D., 2013. Adaptive laboratory evolution - principles and applications for biotechnology. Microb. Cell Fact. 12:64. https://doi.org/10.1186/1475-2859-12-64

Dürre, P., 2016. Physiology and sporulation in clostridium. Bact. Spore From Mol. to Syst. 313–329. https://doi.org/10.1128/9781555819323.ch15

Ewels, P., Magnusson, M., Lundin, S., Käller, M., 2016. MultiQC: Summarize analysis results for multiple tools and samples in a single report. Bioinformatics 32, 3047–3048. https://doi.org/10.1093/bioinformatics/btw354

Fackler, N., Heijstra, B.D., Rasor, B.J., Brown, H., Martin, J., Ni, Z., Shebek, K.M., Rosin, R.R., Simpson, S.D., Tyo, K.E., Giannone, R.J., Hettich, R.L., Tschaplinski, T.J., Leang, C., Brown, S.D., Jewett, M.C., Köpke, M., 2021. Stepping on the Gas to a Circular Economy: Accelerating Development of Carbon-Negative Chemical Production from Gas Fermentation. Annu. Rev. Chem. Biomol. Eng. 12, 439–470. https://doi.org/10.1146/annurev-chembioeng

Fimlaid, K.A., Jensen, O., Donnelly, M.L., Francis, M.B., Sorg, J.A., Shen, A., 2015. Identification of a Novel Lipoprotein Regulator of *Clostridium difficile* Spore Germination. PLOS Pathog. 11:e1005239. https://doi.org/10.1371/JOURNAL.PPAT.1005239

Fong, S.S., Joyce, A.R., Palsson, B., 2005. Parallel adaptive evolution cultures of *Escherichia coli* lead to convergent growth phenotypes with different gene expression states. Genome Res. 15, 1365–1372. https://doi.org/10.1101/gr.3832305

Gassler, T., Sauer, M., Gasser, B., Egermeier, M., Troyer, C., Causon, T., Hann, S., Mattanovich, D., Steiger, M.G., 2020. The industrial yeast *Pichia pastoris* is converted from a heterotroph into an autotroph capable of growth on CO_2. Nat. Biotechnol. 38, 210–216. https://doi.org/10.1038/s41587-019-0363-0

Gleizer, S., Ben-Nissan, R., Bar-On, Y.M., Antonovsky, N., Noor, E., Zohar, Y., Jona, G., Krieger, E., Shamshoum, M., Bar-Even, A., Milo, R., 2019. Conversion of *Escherichia coli* to Generate All Biomass Carbon from CO_2. Cell 179, 1255-1263.e12. https://doi.org/10.1016/j.cell.2019.11.009

Good, B.H., McDonald, M.J., Barrick, J.E., Lenski, R.E., Desai, M.M., 2017. The dynamics of molecular evolution over 60,000 generations. Nature 551, 45–50. https://doi.org/10.1038/nature24287

Harris, L.M., Welker, N.E., Papoutsakis, E.T., 2002. Northern, morphological, and fermentation analysis of *spo0A* inactivation and overexpression in *Clostridium acetobutylicum* ATCC 824. J. Bacteriol. 184, 3586–3597. https://doi.org/10.1128/JB.184.13.3586-3597.2002

Helling, R.B., Vargas, C.N., Adams, J., 1987. Evolution of *Escherichia coli* during growth in a constant environment. Genetics 116, 349–358. https://doi.org/10.1093/genetics/116.3.349

Humphreys, C.M., McLean, S., Schatschneider, S., Millat, T., Henstra, A.M., Annan, F.J., Breitkopf, R., Pander, B., Piatek, P., Rowe, P., Wichlacz, A.T., Woods, C., Norman, R., Blom, J., Goesman, A., Hodgman, C., Barrett, D., Thomas, N.R., Winzer, K., Minton, N.P., 2015. Whole genome sequence and manual annotation of *Clostridium autoethanogenum*, an industrially relevant bacterium. BMC Genomics 16:1085. https://doi.org/10.1186/s12864-015-2287-5

IEA, 2022. World Energy Outlook 2022. https://www.iea.org/reports/world-energy-outlook-2022

IPCC, 2021. Climate Change 2021: the Physical Science Basis. Contribution of Working Group I to the Sixth Assessment Report of the Intergovernmental Panel on Climate Change.

Jin, S., Kang, S., Bae, J., Lee, H., Cho, B.-K., 2022. Development of CO gas conversion system using high CO tolerance biocatalyst. Chem. Eng. J. 449:137678. https://doi.org/10.1016/j.cej.2022.137678

Kang, S., Song, Y., Jin, S., Shin, J., Bae, J., Kim, D.R., Lee, J.-K., Kim, S.C., Cho, S., Cho, B.K., 2020. Adaptive Laboratory Evolution of *Eubacterium limosum* ATCC 8486 on Carbon Monoxide. Front. Microbiol. 11:402. https://doi.org/10.3389/fmicb.2020.00402

Kircher, M., 2021. Bioeconomy – present status and future needs of industrial value chains. N. Biotechnol. 60, 96–104. https://doi.org/10.1016/j.nbt.2020.09.005

Klask, C., Kliem-Kuster, N., Molitor, B., Angenent, L.T., 2020. Nitrate Feed Improves Growth and Ethanol Production of *Clostridium ljungdahlii* With CO_2 and H_2, but Results in Stochastic Inhibition Events. Front. Microbiol. 11:724. https://doi.org/10.3389/fmicb.2020.00724

Kolek, J., Diallo, M., Vasylkivska, M., Branska, B., Sedlar, K., López-Contreras, A.M., Patakova, P., 2017. Comparison of expression of key sporulation, solventogenic and acetogenic genes in *C. beijerinckii* NRRL B-598 and its mutant strain overexpressing *spo0A*. Appl. Microbiol. Biotechnol. 101, 8279–8291. https://doi.org/10.1007/s00253-017-8555-3

Köpke, M., Simpson, S.D., 2020. Pollution to products: recycling of 'above ground' carbon by gas fermentation. Curr. Opin. Biotechnol. 65, 180–189. https://doi.org/10.1016/j.copbio.2020.02.017

Kwon, S.J., Lee, J., Lee, H.S., 2022. Metabolic changes of the acetogen Clostridium sp. AWRP through adaptation to acetate challenge. Front. Microbiol. 13, 982442. https://doi.org/10.3389/FMICB.2022.982442

LaCroix, R.A., Sandberg, T.E., O'Brien, E.J., Utrilla, J., Ebrahim, A., Guzman, G.I., Szubin, R., Palsson, B.O., Feist, A.M., 2015. Use of adaptive laboratory evolution to discover key mutations enabling rapid growth of *Escherichia coli* K-12 MG1655 on glucose minimal medium. Appl. Environ. Microbiol. 81, 17–30. https://doi.org/10.1128/AEM.02246-14

Lemaire, O.N., Jespersen, M., Wagner, T., 2020. CO_2-Fixation Strategies in Energy Extremophiles: What Can We Learn From Acetogens? Front. Microbiol. 11, 1–8. https://doi.org/10.3389/fmicb.2020.00486

Lemaire, O.N., Wagner, T., 2021. Gas channel rerouting in a primordial enzyme: Structural insights of the carbon-monoxide dehydrogenase/acetyl-CoA synthase complex from the acetogen *Clostridium*

autoethanogenum. Biochim. Biophys. Acta - Bioenerg. 1862, 148330. https://doi.org/10.1016/j.bbabio.2020.148330

Li, H., Handsaker, B., Wysoker, A., Fennell, T., Ruan, J., Homer, N., Marth, G., Abecasis, G., Durbin, R., 2009. The Sequence Alignment/Map format and SAMtools. Bioinformatics 25, 2078–2079. https://doi.org/10.1093/BIOINFORMATICS/BTP352

Li, Q., Chen, J., Minton, N.P., Zhang, Y., Wen, Z., Liu, J., Yang, H., Zeng, Z., Ren, X., Yang, J., Gu, Y., Jiang, W., Jiang, Y., Yang, S., 2016. CRISPR-based genome editing and expression control systems in *Clostridium acetobutylicum* and *Clostridium beijerinckii*. Biotechnol. J. 11, 961–972. https://doi.org/10.1002/BIOT.201600053

Liao, Y., Smyth, G.K., Shi, W., 2019. The R package Rsubread is easier, faster, cheaper and better for alignment and quantification of RNA sequencing reads. Nucleic Acids Res. 47:e47. https://doi.org/10.1093/NAR/GKZ114

Liew, F., Henstra, A.M., Winzer, K., Köpke, M., Simpson, S.D., Minton, N.P., 2016. Insights into CO_2 Fixation Pathway of *Clostridium autoethanogenum* by Targeted Mutagenesis. MBio 7, e00427-16. https://doi.org/10.1128/mBio.00427-16

Liew, F.E., Nogle, R., Abdalla, T., Rasor, B.J., Canter, C., Jensen, R.O., Wang, L., Strutz, J., Chirania, P., De Tissera, S., Mueller, A.P., Ruan, Z., Gao, A., Tran, L., Engle, N.L., Bromley, J.C., Daniell, J., Conrado, R., Tschaplinski, T.J., Giannone, R.J., Hettich, R.L., Karim, A.S., Simpson, S.D., Brown, S.D., Leang, C., Jewett, M.C., Köpke, M., 2022. Carbon-negative production of acetone and isopropanol by gas fermentation at industrial pilot scale. Nat. Biotechnol. 40, 335–344. https://doi.org/10.1038/s41587-021-01195-w

Mahamkali, V., Valgepea, K., Lemgruber, R. de S.P., Plan, M., Tappel, R., Köpke, M., Simpson, S.D., Nielsen, L.K., Marcellin, E., 2020. Redox controls metabolic robustness in the gas-fermenting acetogen *Clostridium autoethanogenum*. Proc. Natl. Acad. Sci. 117, 13168–13175. https://doi.org/10.1073/pnas.1919531117

Martin, M., 2011. Cutadapt removes adapter sequences from high-throughput sequencing reads. EMBnet.journal 17, 10. https://doi.org/10.14806/ej.17.1.200

Martin, M.E., Richter, H., Saha, S., Angenent, L.T., 2015. Traits of selected Clostridium strains for syngas fermentation to ethanol. Biotechnol. Bioeng. 113, 531–539. https://doi.org/10.1002/bit.25827

Mock, J., Zheng, Y., Mueller, A.P., Ly, S., Tran, L., Segovia, S., Nagaraju, S., Köpke, M., Dürre, P., Thauer, R.K., 2015. Energy conservation associated with ethanol formation from H_2 and CO_2 in *Clostridium autoethanogenum* involving electron bifurcation. J. Bacteriol. 197, 2965–2980. https://doi.org/10.1128/JB.00399-15

Oswald, F., Zwick, M., Omar, O., Hotz, E.N., Neumann, A., 2018. Growth and product formation of *Clostridium ljungdahlii* in presence of cyanide. Front. Microbiol. 9:1213. https://doi.org/10.3389/fmicb.2018.01213

Otte, B., Grunwaldt, E., Mahmoud, O., Jennewein, S., 2009. Genome shuffling in *Clostridium diolis* DSM 15410 for improved 1,3-propanediol production. Appl. Environ. Microbiol. 75, 7610–7616. https://doi.org/10.1128/AEM.01774-09

Paredes, C.J., Alsaker, K. V., Papoutsakis, E.T., 2005. A comparative genomic view of clostridial sporulation and physiology. Nat. Rev. Microbiol. 3, 969–978. https://doi.org/10.1038/nrmicro1288

Pavan, M., Reinmets, K., Garg, S., Mueller, A.P., Marcellin, E., Köpke, M., Valgepea, K., 2022. Advances in systems metabolic engineering of autotrophic carbon oxide-fixing biocatalysts towards a circular economy. Metab. Eng. 71, 117–141. https://doi.org/10.1016/j.ymben.2022.01.015

Peebo, K., Valgepea, K., Nahku, R., Riis, G., Õun, M., Adamberg, K., Vilu, R., 2014. Coordinated activation of PTA-ACS and TCA cycles strongly reduces overflow metabolism of acetate in *Escherichia coli*. Appl. Microbiol. Biotechnol. 98, 5131–5143. https://doi.org/10.1007/s00253-014-5613-y

Piatek, P., Olsson, L., Nygård, Y., 2020. Adaptation during propagation improves *Clostridium autoethanogenum* tolerance towards benzene, toluene and xylenes during gas fermentation. Bioresour. Technol. Reports 12, 100564. https://doi.org/10.1016/j.biteb.2020.100564

Rozen, D.E., Lenski, R.E., 2000. Long-Term Experimental Evolution in *Escherichia coli*. VIII. Dynamics of a Balanced Polymorphism. Am. Nat. 155, 24–35. https://doi.org/10.1007/s00239-004-0322-2

Sandberg, T.E., Salazar, M.J., Weng, L.L., Palsson, B.O., Feist, A.M., 2019. The emergence of adaptive laboratory evolution as an efficient tool for biological discovery and industrial biotechnology. Metab. Eng. 56, 1–16. https://doi.org/10.1016/j.ymben.2019.08.004

Schulz, S., Molitor, B., Angenent, L.T., 2023. Acetate augmentation boosts the ethanol production rate and specificity by *Clostridium ljungdahlii* during gas fermentation with pure carbon monoxide. Bioresour. Technol. 369, 128387. https://doi.org/10.1016/J.BIORTECH.2022.128387

Steiner, E., Dago, A.E., Young, D.I., Heap, J.T., Minton, N.P., Hoch, J.A., Young, M., 2011. Multiple orphan histidine kinases interact directly with Spo0A to control the initiation of endospore formation

in *Clostridium acetobutylicum*. Mol. Microbiol. 80, 641–654. https://doi.org/10.1111/j.1365-2958.2011.07608.x

Tremblay, P.L., Höglund, D., Koza, A., Bonde, I., Zhang, T., 2015. Adaptation of the autotrophic acetogen Sporomusa ovata to methanol accelerates the conversion of CO_2 to organic products. Sci. Rep. 5:16168. https://doi.org/10.1038/srep16168

Treves, D.S., Manning, S., Adams, J., 1998. Repeated evolution of an acetate-crossfeeding polymorphism in long-term populations of *Escherichia coli*. Mol. Biol. Evol. 15, 789–797. https://doi.org/10.1093/oxfordjournals.molbev.a025984

Valgepea, K., de Souza Pinto Lemgruber, R., Abdalla, T., Binos, S., Takemori, N., Takemori, A., Tanaka, Y., Tappel, R., Köpke, M., Simpson, S.D., Nielsen, L.K., Marcellin, E., 2018. H_2 drives metabolic rearrangements in gas-fermenting *Clostridium autoethanogenum*. Biotechnol. Biofuels 11, 55. https://doi.org/10.1186/s13068-018-1052-9

Valgepea, K., de Souza Pinto Lemgruber, R., Meaghan, K., Palfreyman, R.W., Abdalla, T., Heijstra, B.D., Behrendorff, J.B., Tappel, R., Köpke, M., Simpson, S.D., Nielsen, L.K., Marcellin, E., 2017a. Maintenance of ATP Homeostasis Triggers Metabolic Shifts in Gas-Fermenting Acetogens. Cell Syst. 4, 505-515.e5. https://doi.org/10.1016/j.cels.2017.04.008

Valgepea, K., Loi, K.Q., Behrendorff, J.B., Lemgruber, R. de S.P., Plan, M., Hodson, M.P., Köpke, M., Nielsen, L.K., Marcellin, E., 2017b. Arginine deiminase pathway provides ATP and boosts growth of the gas-fermenting acetogen *Clostridium autoethanogenum*. Metab. Eng. 41, 202–211. https://doi.org/10.1016/j.ymben.2017.04.007

Valgepea, K., Talbo, G., Takemori, N., Takemori, A., Ludwig, C., Mahamkali, V., Mueller, A.P., Tappel, R., Köpke, M., Simpson, S.D., Nielsen, L.K., Marcellin, E., 2022. Absolute Proteome Quantification in the Gas-Fermenting Acetogen *Clostridium autoethanogenum*. mSystems. 7, e00026-22. https://doi.org/10.1128/msystems.00026-22

Walker, B.J., Abeel, T., Shea, T., Priest, M., Abouelliel, A., Sakthikumar, S., Cuomo, C.A., Zeng, Q., Wortman, J., Young, S.K., Earl, A.M., 2014. Pilon: An integrated tool for comprehensive microbial variant detection and genome assembly improvement. PLoS One. 9:e112963. https://doi.org/10.1371/journal.pone.0112963

Wang, S., Huang, H., Kahnt, J., Mueller, A.P., Köpke, M., Thauer, R.K., 2013. NADP-Specific Electron-Bifurcating [FeFe]-Hydrogenase in a Functional Complex with Formate Dehydrogenase in *Clostridium autoethanogenum* Grown on CO. J. Bacteriol. 195, 4373–4386. https://doi.org/10.1128/JB.00678-13

Wiser, M.J., Ribeck, N., Lenski, R.E., 2013. Long-Term Dynamics of Adaptation in Asexual Populations. Science. 342, 1364–1367. https://doi.org/10.1126/science.1243357

Xin, X., Cheng, C., Du, G., Chen, L., Xue, C., 2020. Metabolic Engineering of Histidine Kinases in *Clostridium beijerinckii* for Enhanced Butanol Production. Front. Bioeng. Biotechnol. 8:214. https://doi.org/10.3389/fbioe.2020.00214

Xu, M., Zhao, J., Yu, L., Tang, I.C., Xue, C., Yang, S.T., 2015. Engineering *Clostridium acetobutylicum* with a histidine kinase knockout for enhanced n-butanol tolerance and production. Appl. Microbiol. Biotechnol. 99, 1011–1022. https://doi.org/10.1007/s00253-014-6249-7

Zhang, J., Guo, L., Gao, C., Song, W., Wu, J., Liu, L., Xiulai, C., 2022. Metabolic engineering strategies for microbial utilization of C1 feedstocks. Syst. Microbiol. Biomanufacturing. 3, 122–136. https://doi.org/10.1007/S43393-022-00135-2